ARTICLES

Optical and photoelectrical studies of charge-transfer processes in $YAlO_3$:Ti crystals

S. A. Basun
A. F. Ioffe Physicotechnical Institute, Academy of Sciences of Russia, 194021, St. Petersburg, Russia

T. Danger
Institut für Laser-Physik, Universitat Hamburg, Jungiusstrasse 9a, D-20355 Hamburg, Germany

A. A. Kaplyanskii
A. F. Ioffe Physicotechnical Institute, Academy of Sciences of Russia, 194021, St. Petersburg, Russia

D. S. McClure
Department of Chemistry, Princeton University, Princeton, New Jersey 08544

K. Petermann
Institut für Laser-Physik, Universitat Hamburg, Jungiusstrasse 9a, D-20355 Hamburg, Germany

W. C. Wong
Department of Chemistry, Princeton University, Princeton, New Jersey 08544
(Received 14 September 1995; revised manuscript received 24 April 1996)

The donor and acceptor charge-transfer transitions in $YAlO_3$:Ti^{3+}/Ti^{4+} were investigated through absorption, emission, excitation, one-photon and two-photon photoconductivities, excited-state absorption, and thermoluminescence. The results are contrasted to similar studies previously made on Al_2O_3:Ti^{3+}/Ti^{4+}. The dominant Ti^{3+} population has a photoionization threshold at 37 000 cm^{-1}. The lowest energy Ti^{4+} charge-transfer transition has its zero-phonon energy near to 33 900 cm^{-1}. The sum of these two quantities agrees with the reported band-gap energy of $YAlO_3$. The position of the Ti^{3+}/Ti^{4+} level in the band gap of $YAlO_3$ is determined by these measurements. Stimulated emission from the ^2E state of Ti^{3+} is limited by photoionization from this state. [S0163-1829(96)05433-1]

I. INTRODUCTION

$YAlO_3$ crystallizes in a slightly distorted perovskite structure; the space group was determined to be orthorhombic $Pnma$ (D_{2h}^{16}).[1] In $YAlO_3$ crystals doped with Ti, both trivalent Ti^{3+} and tetravalent Ti^{4+} ions are incorporated into the lattice; the concentration ratio Ti^{3+}/Ti^{4+} depends on the crystal-growth conditions. The optical properties of $YAlO_3$:Ti^{3+} were studied in several papers.[2–8] The optical spectra of $Ti^{3+}(3d^1)$ ions substituting in the $YAlO_3$ lattice for the Al^{3+} in octahedral oxygen coordination were identified. The simple energy scheme of a $3d^1$ ion in an octahedral field consists of only two electronic states ^2T (lowest) and ^2E. Transitions from the ground state $^2T \rightarrow {}^2E$ give in the absorption spectrum a broad vibronic Jahn-Teller split band with two peaks (432 and 491 nm). The back transition from the metastable state $^2E \rightarrow {}^2T$ gives a broad vibronic luminescence band with maximum at 610 nm and the most prominent zero-phonon line (ZPL) at 18 530 cm^{-1} (one of the three which are theoretically possible).[6] The idea to use the broad vibronic $^2E \rightarrow {}^2T$ band transitions in $YAlO_3$:Ti^{3+} for creation of a tunable solid-state laser operating in the short-wavelength visible range strongly attracted attention to the properties of $YAlO_3$:Ti crystals.[2,3,9,10] It was found[2,3] however that lasing is suppressed in $YAlO_3$:Ti because of intense excited-state absorption (ESA) from the metastable ^2E state of Ti^{3+}. Ti^{3+} itself has no levels above ^2E, hence the ESA transitions should belong to highly excited states of charge-transfer (CT) type that are connected with the host lattice. These states may be either delocalized conductive states of ''free carriers'' in conduction bands or localized states of ''bound exciton'' type[11] when, say, the electron is transferred from Ti^{3+} to the surrounding metal ligands, being bound in an attractive Coulomb field of the remaining photoionized charged ion (Ti^{4+}). The CT transitions to some lattice defects have to be considered too.

In the present paper, charge-transfer transitions in $YAlO_3$:Ti crystals, which have different relative amounts of Ti^{3+}/Ti^{4+}, were studied by several techniques. We have measured (i) ground-state absorption (GSA) spectra in the UV region, which correspond to relatively high energies of CT optical transitions, (ii) UV excited blue emission and the corresponding excitation spectra of Ti^{4+} at liquid-nitrogen temperature (LNT), (iii) UV excitation spectra of the intrinsic $^2E \rightarrow {}^2T$ luminescence of Ti^{3+} ions, (iv) photoconductivity excited both in the UV region in a one-photon process

and in the visible in two- (or three-) step photoionization processes via the metastable ^2E state of Ti^{3+}, which gives direct information on the photoexcitation of conductive CT states, (v) UV excitation spectra of thermoluminescence (TL), which gives additional information on the carriers produced by UV light.

The CT transitions of donor type and of acceptor type were identified in the spectra of $YAlO_3$:Ti. These correspond to photoionization of Ti with the creation of electrons in conduction band (CB) or holes in valence band (VB), respectively. On the basis of the experimental observations, an energy scheme of the system $YAlO_3$:Ti was constructed showing the position of the energy level Ti^{3+}/Ti^{4+} in the $YAlO_3$ band gap.

II. EXPERIMENT AND RESULTS

The samples of $YAlO_3$:0.2% Ti (nominal concentration) with different relative amounts of Ti^{3+}/Ti^{4+} were grown at Hamburg by the Czochralski method in reducing atmosphere (5% H_2, 95% Ar) or in oxidizing atmosphere (1% O_2, 99% N_2). In samples grown in oxidizing atmosphere, the amount of Ti^{4+} ions is especially high, as in samples codoped with divalent metal ions (Mn). A boule of $YAlO_3$:0.02% Ti (nominal concentration) was given to us by M. Kokta of Union Carbide Corporation and samples were cut from it. Although the relative intensities of the absorption bands are different in the differently grown $YAlO_3$:Ti, it can be seen from below that the positions of the bands are all identical. Also, the photoconductivity spectra of the samples with different amounts of Ti^{3+} and Ti^{4+} are qualitatively the same. This makes it valid to relate the optical and photoelectrical properties of different crystals. Semiquantitative estimates of the Ti^{3+}/Ti^{4+} ratios in the different samples were made.

A. UV absorption spectra

The GSA spectrum of $YAlO_3$:Ti in the UV consists of several broad bands whose relative intensities depend strongly on the relative amount of Ti^{3+} and Ti^{4+} ions in the sample. Figure 1 shows the GSA spectra of several differently grown doped and undoped samples in the UV region. The UV1 band, with a long-wavelength onset at ~340 nm and a maximum at 280 nm, was described previously in Ref. 3. This band is intense in the GSA of a $YAlO_3$:Ti sample grown in a reducing atmosphere where the Ti^{3+} valence state is dominant. The intensity of UV1 drops dramatically in the GSA of $YAlO_3$:Ti samples grown in oxidizing atmosphere, which contain mainly Ti^{4+} and only a small amount of Ti^{3+} ions. In the GSA of the latter samples, the UV2 band has its onset at 280 nm and it has a peak at 215 nm and a shoulder at 235 nm. The steep incline at wavelengths shorter than 200 nm (''UV3 band'') observed for the mainly Ti^{3+} doped samples is at least very small for the mainly Ti^{4+}-doped crystals. For comparison, undoped $YAlO_3$ crystals grown under reducing and oxidizing conditions were also investigated. These show only small residual absorptions between 350 and 190 nm. Table I summarizes the spectral parameters of individual UV bands and their phenomenological relation to the presence of particular ions in the sample — Ti^{3+} (UV1, UV3) and Ti^{4+} (UV2). The intensities of these bands relative to the visible band were estimated from the absorption peaks and from corrected excitation spectra, and are also given in Table I.

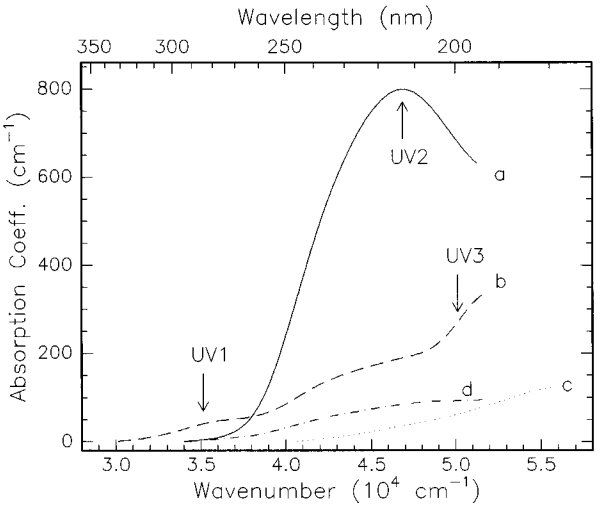

FIG. 1. UV absorption spectra of 0.2% (nominal concentration) Ti-doped (a,b) and undoped (c,d) $YAlO_3$ crystals (Hamburg) grown in oxidizing atmosphere (a,c) or in reducing atmosphere (b,d). $T=300$ K. UV1, UV3 belong to Ti^{3+}, UV2 to Ti^{4+}.

TABLE I. Absorption bands of $YAlO_3$:Ti.

	Long-wavelength edge	Band maximum or shoulder	Related to the presence of	Relative integrated absorption strengths
VIS	560 nm ~18 000 cm^{-1}	440,490 nm ~23 000,20 000 cm^{-1}	Ti^{3+}	1
UV1	340 nm ~29 000 cm^{-1}	280 nm ~36 000 cm^{-1}	Ti^{3+}	50
UV2	280 nm ~36 000 cm^{-1}	215,235 nm ~46 500,42 600 cm^{-1}	Ti^{4+}	850
UV3	~220 nm ~45 000 cm^{-1}	175 nm ~57 000 cm^{-1}	Ti^{3+}	~300

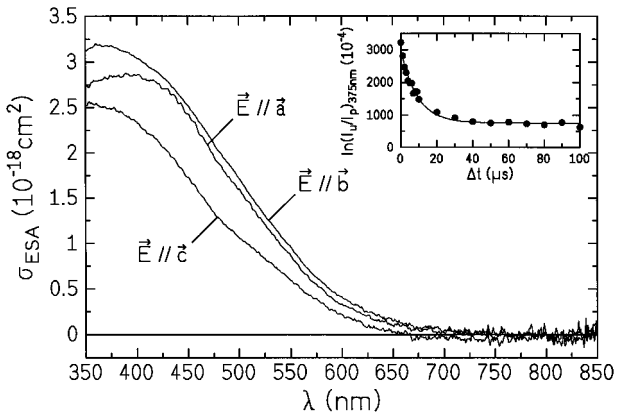

FIG. 2. Polarized ESA cross sections, σ_{ESA} of $YAlO_3$:Ti^{3+} (0.2% Ti doped). In the inset the temporal behavior of the unpolarized pump-induced absorption is shown. I_p and I_u are the transmitted probe beam intensities with and without excitation, Δt is the trigger delay between the pump and probe pulse.

B. Excited-state absorption

The excited-state absorption (ESA) of $YAlO_3$:Ti was measured using the pump and probe technique described in Ref. 8. An excimer-laser-pumped dye laser at 488 nm wavelength was used as pump source. The ESA of $YAlO_3$:Ti hardly depends on the orientation of the crystal (Fig. 2). The ESA cross sections, σ_{ESA}, at the pump wavelengths of the order of 10^{-18} cm^2 are about 50 times larger than those for GSA. The long-wavelength edge of the ESA also affects the short-wavelength emission region. No stimulated emission could be detected in the whole fluorescence range.[8] The decay time of the ESA determined by time-resolved ESA measurements is about 10 μs, which is in good agreement with the ^2E lifetime of Ti^{3+} in $YAlO_3$ of 11.4 μs. In addition, a long-lived pump-induced absorption attributed to color centers occurs. The fraction of this component with a decay time of a few milliseconds and a long-wavelength edge shifted to the blue spectral range (by 50 nm) compared to the ESA is roughly 20% of the total transient absorption at the peak wavelength of 375 nm (Fig. 2).[8]

C. UV excited emission and excitation spectra of Ti^{4+}

The 260 nm excited emissions at LNT consist of both the *d-d* yellow band and a broad blue band peaking at 410 nm. In the Union Carbide $YAlO_3$:Ti, the intensity of the blue emission is comparable to the *d-d* emission. In the Hamburg $YAlO_3$:Ti, which has less Ti^{4+}, the blue emission is only one-tenth as intense as the *d-d* emission. The lifetimes of the blue emissions excited at 266 nm are found to be 13.9 ± 2.0 μs and 5.8 ± 0.6 μs at 87 K. These values are about 100 times less than that in Al_2O_3:Ti.[12] Also, unlike the blue emission in Al_2O_3:Ti, the 410 nm emission band in $YAlO_3$:Ti can barely be detected at RT. These facts can be explained as being caused by a rapid nonradiative process from the emitting level, contrary to the case of Al_2O_3:Ti^{4+}.[13]

After the *d-d* band is subtracted from the spectrum, the blue emission is plotted in Fig. 3. The excitation spectrum of an optically dense sample of the Union Carbide crystal measured at 420 nm is also shown in the same figure.

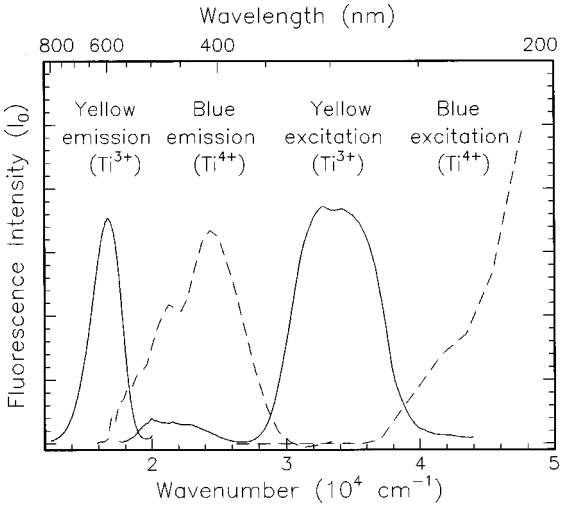

FIG. 3. Dashed curve: 260 nm excited blue emission spectrum of $YAlO_3$:0.02% Ti (*d-d* emission band subtracted) and the excitation spectrum measured at 420 nm. Both are taken at LNT. (Union Carbide sample). Solid curve: 300 nm excited yellow emission spectrum and its excitation spectrum detected at 600 nm at RT.

D. Excitation spectra of Ti^{3+} fluorescence

A comparison between the photoluminescence (PL) spectra of different samples at 2 K shows that in the ZPL spectral region, all spectra are totally identical and contain only one ZPL at 18 530 cm^{-1}. We could conclude that only one type of Ti^{3+} center manifests itself in this region of PL. However, the bandwidth (full width at half maximum) of the ZPL is 5 cm^{-1} and must be due to an inhomogeneous distribution of some type. The excitation spectrum of the intrinsic $^2E\rightarrow{}^2T$ fluorescence of Ti^{3+} ions was measured using a color filter selecting ''yellow'' luminescence of the samples (measuring about 600 nm). In accordance with Ref. 3, the excitation spectrum in the visible consists of the band with two peaks, which unambiguously corresponds to direct excitation of Ti^{3+} ions in the $^2T\rightarrow{}^2E$ absorption band. In the near UV, a broad maximum is observed in the region of the UV1 absorption band (see Fig. 3).[3] Further in the UV, the excitation spectrum shows a steep drop in the region of the UV2 band.

The excitation spectrum in the UV1 range of Fig. 3 corresponds to a ''thick sample'' excitation spectrum in which almost all of the exciting light is absorbed over much of the band. The height of the 300 nm excitation band corresponding to UV1 should be multiplied by a factor of 4 to 5 to show its true strength relative to the *d-d* excitation band for the crystal sample used, namely the 1.55 mm thick sample from Union Carbide.

E. Photoelectric response in UV

The stationary photocurrent (PC) of $YAlO_3$:Ti was measured using the technique described in Ref. 14, but without insulating plates between the Ni mesh electrodes and the sample. The results are generally in accordance with earlier measurements.[15] Under UV excitation, we observed the low-energy step threshold of the spectral PC tail at $\sim$32 000 cm^{-1}. At room temperature it is approximately three times

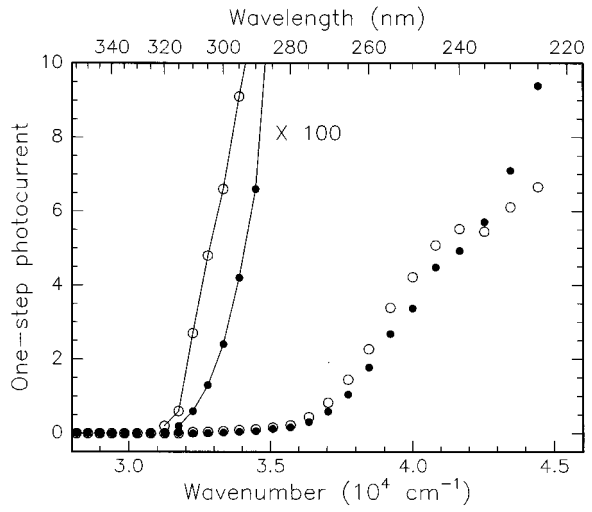

FIG. 4. Excitation spectrum of one-step photocurent in the UV region at RT (open circles) and LNT (solid circles) for the $YAlO_3$:0.02% Ti. (Union Carbide sample).

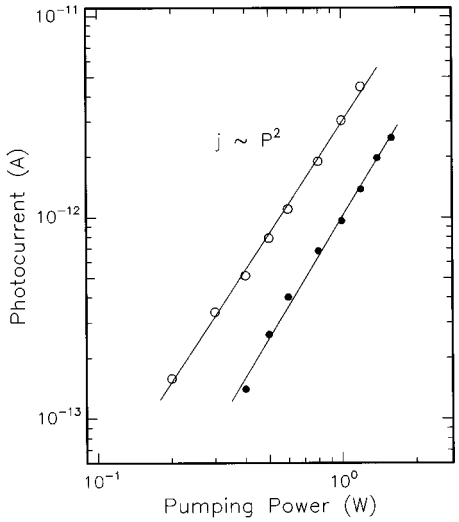

FIG. 5. Dependence of stationary two-step photocurrent on visible excitation (λ_{exc}=488 nm). Field strength, E=100 kV/cm, T=77 K. Open circles are $YAlO_3$:0.2% Ti, solid circles are $YAlO_3$:0.2% Ti, 0.1% Mn.

stronger than at 77 K (see Fig. 4). The photocurrent increases with frequency. Especially fast increases in slope begin at ~37 000 and ~44 000 cm^{-1}. The photocurrent in these regions is 50–100 times stronger than in the first region (Fig. 4), and its temperature dependence is much less.

F. Photoelectric response in visible range

The previous measurements of photocurrent in Ti^{3+}-doped oxides Al_2O_3 and YAG revealed the possibility of excitation of photoconductivity under visible excitation when the photocurrent appears as a result of two-step photoionization of Ti^{3+} via its intermediate ^2E state.[16,17] Because the first step is well known here as the intrinsic excitation $^2T \rightarrow {}^2E$ of the Ti^{3+} ion, this helps in the identification of final states in the two-step or the corresponding one-step transitions.

In the present studies of two-step photocurrent in $YAlO_3$:Ti crystals (see also Ref. 18), the cw Ar laser spectral lines 457.9–514.5 nm corresponding to energies at 19 440–21 840 cm^{-1} were used for excitation. These lines are situated within the $^2T \rightarrow {}^2E$ absorption band of Ti^{3+} and hence effectively excite Ti^{3+} into the metastable ^2E state, which is 18 530 cm^{-1} above the ^2T ground state. Inducing the second-step transition from ^2E (18 530 cm^{-1}), these lines excite the system to upper energy states at 37 970–40 370 cm^{-1}. These correspond to the high-energy falling edge of the UV1 band and its crossover to UV2 in the GSA of $YAlO_3$:Ti (see Fig. 1).

Figure 5 shows the dependence of the stationary photocurrent j on the cw Ar laser pumping power P at LNT. These dependences were measured for two samples with the same Ti concentration grown under reducing atmosphere where Ti^{3+} ions dominate: the sample $YAlO_3$:0.2% Ti and codoped sample $YAlO_3$:0.2% Ti, 0.1% Mn with an enhanced concentration of Ti^{4+} ions. The quadratic dependence $j(P)$ is observed in both cases and for all excitation wavelengths, the current in the codoped sample being smaller. The quadratic dependence establishes that the two-step photoionization of Ti^{3+} ions by visible light creates electrons in the conduction band (CB): $Ti^{3+} + 2h\nu \rightarrow Ti^{4+} + e^-$. The stationary current is $j \sim Gl \sim Gn_r^{-1}$ where $G \sim P^2$ is the rate of photoionization in the two-step process, and $l \sim n_r^{-1}$ is the mean free path of a charge carrier between the generation and recombination events, n_r being the concentration of recombination centers.[19] Since the photocurrent is due to electrons, the decrease of current in the Ti^{4+}-enriched sample suggests that Ti^{4+} ions serve as recombination centers ($Ti^{4+} + e^- \rightarrow Ti^{3+}$), however more samples are needed to establish the actual dependence of photocurrent of n_r.

In Fig. 6, the wavelength dependence of the relative photoionization cross section from the ^2E level of Ti^{3+} is plotted, that is,

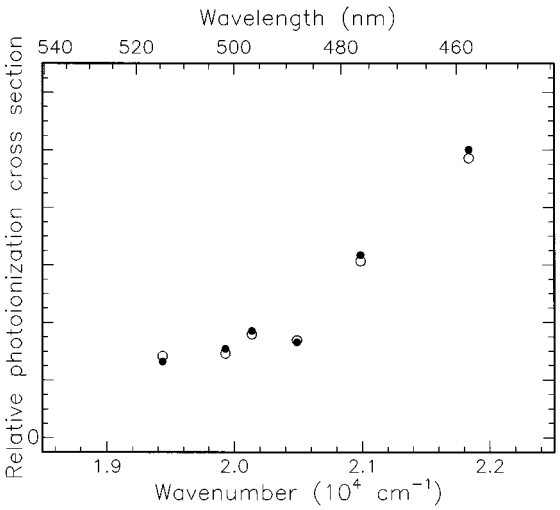

FIG. 6. Relative second-step photoionization cross section from ^2E state of Ti^{3+} versus pump wavelength at 77 K. Open circles are $YAlO_3$:0.2% Ti, solid circles are $YAlO_3$:0.2% Ti, 0.1% Mn.

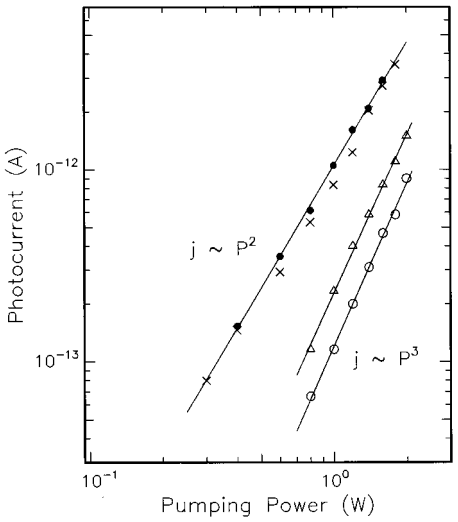

FIG. 7. Photocurrent versus pump power for $YAlO_3$:0.2% Ti, 0.1% Mn samples at $T=2$ K. $E=100$ kV/cm, $\lambda_{exc}=457.9$ nm (solid circles), 476.5 nm (crosses), 488 nm (triangles), and 514.5 nm (open circles). The triangles and open circles are shifted by a factor of 2 downward.

$$\sigma_{pi}(\nu)\sim\frac{j(\nu)h\nu}{n_i(\nu)P}. \tag{1}$$

Here, n_i is the density of the excited Ti^{3+} ions determined to within a constant factor by recording the $^2E\rightarrow{}^2T$ spontaneous fluorescence intensity in parallel to the two-step photocurrent, j, and P is the incident power of 0.5 W at each cw Ar laser line. It is seen that there is a change of photoionization cross section at about 20 500 cm^{-1}.

If the samples are cooled from LNT down to liquid-helium temperature (LHT), a different power dependence of the photocurrent is observed (Fig. 7). While the quadratic dependence $j(P)$ remains for short-wavelength Ar laser lines, for excitation with the longer wavelength lines (488 and 514 nm), the pump power dependence of photocurrent becomes cubic ($j\sim P^3$). The spectral point of crossover, $j\sim P^2\rightarrow j\sim P^3$, is between 488 and 476 nm (20 500–21 000 cm^{-1}) and corresponds to that energy at which the photoionization cross section from the ^2E state, $\sigma_{pi}(\nu)$, increases abruptly (see Fig. 6). The corresponding one-photon energy of this excitation point is at about 39 000 cm^{-1}. These changes in $j(P)$ are observed on all reduced and Mn codoped samples.

G. UV excitation spectra of thermoluminescence

The photon counts of the *d-d* luminescence were measured after UV excitation of the sample at 80 K in the course of subsequent relatively slow heating (~4 K/min) of the sample up to 400 K. When a blue filter was used, no TL peaks were detected. Four major thermoluminescence (TL) peaks were observed (Fig. 8). The dependences of individual TL peak amplitudes on the exciting UV frequency (normalized to the UV source output) were measured (the TL excitation spectrum, TLES). Two types of TLES were observed (Fig. 9). TLES-1 measured for the TL peak at 280 K contains a UV maximum and has a low-energy threshold which coincides with the weak PC tail threshold at 32 000 cm^{-1}. The energetic depth of this trap is estimated to be about 0.56 eV according to the empirical formula $\Delta E\approx T_{max}/500$. Towards high energy, TLES-1 drops at ~37 000 cm^{-1}, where the other TL peaks (TLES-2) begin. TLES-2 is observed for all other TL peaks. It begins at ~37 000 cm^{-1} when TLES-1 starts to decrease. The amplitude of TLES-2 increases with frequency.

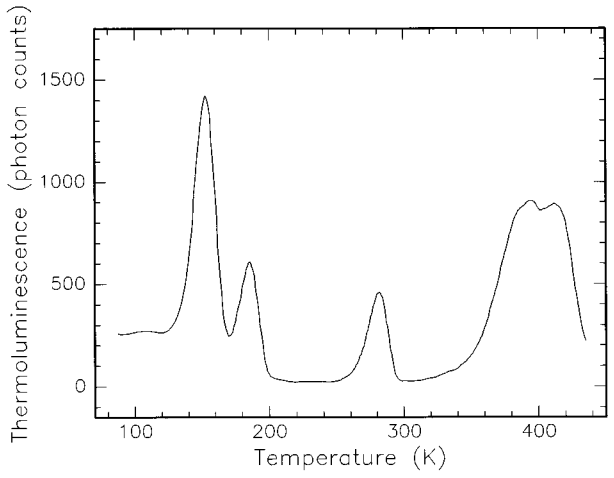

FIG. 8. Thermoluminescence peaks of the *d-d* emission (through at 550 nm cutoff filter) after irradiation of $YAlO_3$:0.02% Ti at 80 K by 265 nm light (heating rate ~4 K/min).

Because the TL peaks arise from the thermal release of photogenerated carriers from traps in the lattice, the observation of two types of TLES indicates the existence of two kinds of ionization processes (with different onset energies) producing electrons that are subsequently captured by several types of traps at LNT.

III. DISCUSSION

The experimental data in Sec. II show that in $YAlO_3$:Ti spectra, besides the internal *d-d* transitions of Ti^{3+} ions in the visible, optical transitions of the charge-transfer (CT) type occur in the UV. These transitions manifest themselves first of all in the UV ground-state absorption spectra (GSA) as well as in the UV excitation spectra of photoluminescence

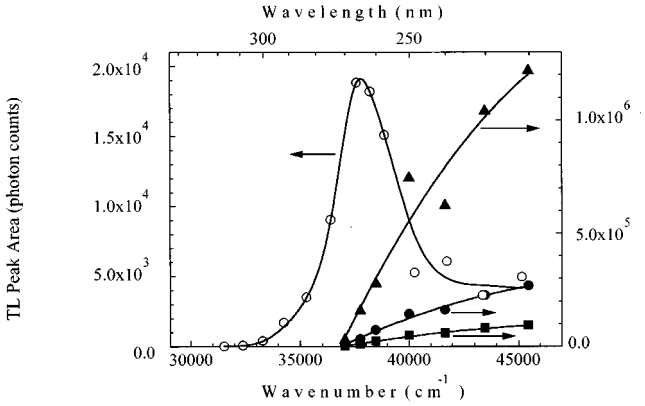

FIG. 9. Excitation spectra of thermoluminescence peaks for $YAlO_3$:0.02% Ti (a) TLES-1 280 K (open circles), (b) TLES-2 [150 K (solid circles), 182 K (squares), 400 K (triangles)].

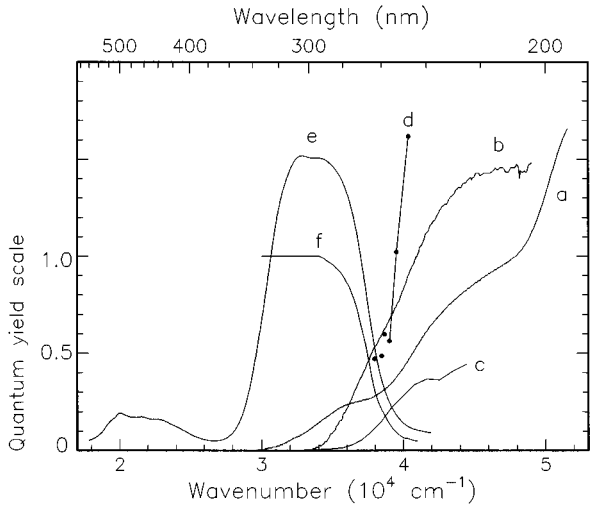

FIG. 10. Excitation spectra in near UV region (summary based on previous figures). (a) GSA of the sample containing Ti^{3+}, Ti^{4+} ions (Fig. 1). (b) ESA (Fig. 2), shifted by 18 530 cm^{-1}. (c) one-step PC (Fig. 4). (d) photoionization cross section from ^2E (Fig. 6), shifted by 18 530 cm^{-1}. (e) excitation of Ti^{3+} PL (Fig. 3), RT. (f) quantum yield of yellow fluorescence, RT.

(PL), of photoconductivity (PC), and of thermoluminescence (TL). In the following, the possible nature of the different CT excited states is discussed for optical transitions in the region of the principal UV absorption bands (UV1, UV2) which are due to the presence of Ti^{3+} and Ti^{4+} in the $YAlO_3$ lattice.

Due to a strong electron-phonon coupling and the fact that the final states may be continuous band states, the CT spectral bands are very broad. As a result of the overlapping between these spectral bands of different origin, it is difficult to determine precisely the spectroscopic parameters such as the positions of low-energy edges of these spectral bands and the corresponding pure-electron transition energies (ZPL's). Therefore, the experimental data only allow us to construct a general and crude scheme for the optical CT transitions in $YAlO_3$:Ti between the Ti levels and the host conduction- (CB) and valence-band (VB) states.

A. Absorption band UV1 and donor-type CT transitions in $YAlO_3$:Ti

As shown in Sec. II A, the GSA band UV1 is intense in the predominantly Ti^{3+} $YAlO_3$ and absent in the predominantly Ti^{4+} crystal. Hence, this band is attributed to the presence of the Ti^{3+} ion and belongs to the dominant type of Ti^{3+} containing centers in $YAlO_3$. Photoexcitation of this band leads to the yellow $^2E \rightarrow {}^2T$ luminescence of Ti^{3+} as it should if it is a Ti^{3+} band. Figure 10 summarizes the data on the UV absorption (GSA) and on the UV excitation spectra of Ti^{3+} PL, of PC, and of TL in the region of the UV1 band. The RT visible spectra (ESA and PC) arising from the CT transitions from the metastable ^2E state of Ti^{3+} are also shown after being shifted by the ^2E energy of 18 530 cm^{-1}. Analogously to Al_2O_3:Ti, all of these results are in agreement with the assignment of UV1 as a titanium-bound exciton.[20]

The Ti-bound exciton must also be reached in the two-step ESA transition. The ESA band appears to begin at about 15 400 cm^{-1}, or 33 900 cm^{-1} above the ground state. This energy is just below the peak energy of UV1 and about 4 000 cm^{-1} above the origin of UV1. A shoulder can be seen in the $E \| c$ ESA spectrum at 480 nm or 39 300 cm^{-1} above the ground state, that is, about 4000 cm^{-1} above the peak of UV1. Therefore, this first part of the ESA band appears to correspond to the UV1 band, but shifted 4000 cm^{-1} to higher energy. A possible reason for such a shift, as was invoked for Al_2O_3:Ti,[12] is that the Jahn-Teller effect in the ^2E state causes a Franck-Condon shift of 4000 cm^{-1} in the transition from ^2E to the exciton state.

However, some differences between $YAlO_3$:Ti and Al_2O_3:Ti are worth mentioning here. The quantum yield of the *d-d* luminescence excited from the exciton band at 300 K is very high in $YAlO_3$, but very low in Al_2O_3. On the other hand, the quantum yield of the blue luminescence excited from the oxygen to metal charge-transfer band at 300 K is high in Al_2O_3 but very low in $YAlO_3$. We have no simple explanation for these facts. The exciton band in $YAlO_3$ has a full width at half height of 8000 cm^{-1}, twice as large as in Al_2O_3. This difference may be related to the more complex band structure of $YAlO_3$ in which two types of cations contribute electronic levels, or to two different types of Ti^{3+} centers. A third point of interest is that the ratio of the *d-d* intensity to the exciton intensity is 1/50 in $YAlO_3$ and 1/2 in Al_2O_3. Information like this for a variety of other host lattices may lead to a better understanding of the charge-transfer processes.

In $YAlO_3$, the intensity of the ESA transition to the exciton state has a cross section of 1.2 to 1.9×10^{-18} cm^2 at 488 nm, depending on the polarization; this is about 50 times greater than the cross section for the *d-d* transition. The ground state to exciton-state transition at 300 nm is also about 50 times stronger than the *d-d* transition; these nearly equal band strengths are in agreement with the assignments of the bands.

The higher-energy part of the ESA band must be due to transitions directly into the conduction band, as the excited-state photoconductivity becomes stronger at wavelengths shorter than 500 nm.

The excitation spectrum in the region of the trapped exciton can be used to find the quantum yield of fluorescence as a function of frequency throughout the band. In the higher-energy part of UV1, photoionization is competing with fluorescence excitation, and the quantum yield of fluorescence should decrease in this region.

The fluorescence yield from a sample plate of thickness d, absorption coefficient a, and quantum yield f is

$$I_F=(I_0-I)f=I_0(1-e^{-ad})f. \tag{2}$$

(Geometry factors can be ignored here.) In our samples, the UV2 band begins to interfere with the UV1 band above 35 000 cm^{-1}, and since UV2 is inactive in producing the yellow fluorescence, its screening effect must be accounted for. This introduces a factor of $a/(a+a')$, where a' is the absorption coefficient of the inactive background adsorption due to UV2. A provisional separation of the contributions of

UV1 and UV2 above 36 000 cm^{-1} was made; UV1 was reflected around 278 nm on a wavelength scale. The quantum yield is then

$$f=\frac{I_F}{I_0}\frac{a+a'}{a}\left(\frac{1}{1-e^{-(a+a')d}}\right). \tag{3}$$

The quantity (I_F/I_0) is taken to be the experimental excitation spectrum and the two correction factors are taken from the absorption spectrum. There is an arbitrary scale factor in the excitation spectrum which must be determined before we can use Eq. (3). We can show that f is the same for the part of UV1 below 34 000 cm^{-1} as for the *d*-*d* band, and we take this value to be $f=1$. Then Eq. (3) can be used to find f for the entire band.

The ratio of absorption peak heights UV 1/*d*-*d* is about 45/1. The excitation spectrum in Fig. 3 shows a ratio of 9.6 to 1, but when the saturation of the excitation spectrum is considered, its peak height should be multiplied by $2.3A/(1-10^{-A})$, where A is the decadic absorbance. At 34 000 cm^{-1}, A for the 1.55 mm Union Carbide sample is 1.73, giving a correction factor of 4.05 and a corrected ordinate height for the excitation band of 39. The ratio of the two excitation bands is thus about 40, nearly the same as the absorption band ratio, and justification for taking $f=1$ at 34 000 cm^{-1}. The photocurrent at this energy is relatively small as shown in Fig. 10, and the high quantum yield shows it to be small absolutely.

Using Eq. (3), the quantum yield is plotted in Fig. 10. It is seen to be constant within 10% from 30 000 to 35 000 cm^{-1}, and then to drop rapidly between 35 000 and 41 000 cm^{-1}. The photocurrent begins to rise at 35 000 and is rising rapidly at 41 000 cm^{-1}. If the photocurrent measured the electron yield p in the conduction band, we should find $f+p=1$. Actually, there is no way to scale the photocurrent to agree with this relation: the current rises faster with frequency than $1-f$, presumably because the electron path length increases with energy above threshold. Any further understanding of this part of the spectrum will have to come from experiments on other crystals in which the effect of UV2 is reduced.

One conclusion of this work is that the weak photocurrent arising at 31 000 cm^{-1} (Fig. 4) does not have a measurable effect on the quantum yield of fluorescence excited in UV1. This observation establishes the scale factor for the weak photocurrent, showing that it is indeed weak. The weak long-wavelength photoconductivity having an onset at 32 000 cm^{-1} coincides with the onset of the TL excitation spectrum for the 280 K glow peak which is interpreted as follows: A special population of Ti^{3+} ions may exist which when illuminated transfer electrons to the trap which has its thermoluminescence peak at 280 K. The other Ti^{3+} ions would not be able to transfer electrons until the higher threshold at 37 000 cm^{-1} has been reached. At still higher energies, the other traps, which are more numerous, will be filled and the excitation spectrum of the 280 K traps shows the falling off due to this competition. It is still necessary to assume that only the 280 K trap is available to the electrons from the special population of Ti^{3+}, and this requires the assumption of some complex consisting of the special Ti^{3+} and 280 K trap which may be a nearby charge-compensated Ti^{4+} ion as it was also assumed in Al_2O_3:Ti.[12]

The results in this section indicate that the photoionization threshold should be at about 37 000 cm^{-1}. However, the extrapolation of the rapid increase of the two-step photocurrent at LNT in Fig. 6 appears to begin at 19 600 cm^{-1} which becomes 38 100 cm^{-1} when ZPL energy is added. Also, the crossover point where the power dependence of the two-step photocurrent changes from quadratic to cubic at LHT is at about 39 000 cm^{-1}. This discrepancy originates from the fact that the two-step processes start from the excited Ti^{3+} level which is displaced relative to the Ti^{3+} ground state. So, a small Franck-Condon shift of about 1000 cm^{-1} is reasonable for the transitions from the ^2E excited state to the conduction band.

B. Absorption band UV2 and acceptor-type CT transitions in $YAlO_3$:Ti

In contrast to UV1 band, UV2 band is prominent in the predominantly Ti^{4+} sample but much weaker in the predominantly Ti^{3+} crystal. So, this band may be attributed to an acceptor-type CT transition of Ti^{4+}, in which an electron from the valence band (VB) is transferred to a Ti^{4+} ion with simultaneous creation of a Ti^{3+} ion in its ground state and a hole in the VB,

$$Ti^{4+}+h\nu_{UV2}\rightarrow Ti^{3+}(^2T)+e^+. \tag{4}$$

The acceptor-type charge-transfer band should have several components because the several molecular orbitals on the oxide ligands are typically spread over an energy range of several volts, and also because of the several *d*-type acceptor orbitals on the Ti ion. Evidence for some of these components appears in the spectrum of Al_2O_3:Ti^{4+}, where two bands about a volt apart are found. The band UV2 in $YAlO_3$:Ti^{4+} appears to be composite; a shoulder can be discerned by Gaussian analysis giving peaks at 238 and 212 nm, a separation of about 0.6 eV. The 238 nm band is more clearly resolved in the excitation spectrum of the blue emission, Fig. 3. The 238 nm band is considered to be the lowest single-singlet transition of the acceptor-type charge transfer. The triplet-singlet transition corresponding to it must give rise to the blue fluorescence because its lifetime is too long to correspond to a spin-allowed transition. The singlet triplet spacing is probably very small, and we have not made a correction for it.

The electronic origin of the Ti^{4+} CT transition can be found from the blue emission band and the corresponding excitation spectrum (Fig. 3). The value obtained from the low-energy excitation edge and the high-energy emission edge is $33\,900\pm1000$ cm^{-1} (4.2 ± 0.1 eV). Taking the average of the 238 nm peak and the emission band peak at 410 nm gives about the same zero-phonon level (33 200 cm^{-1}) as the other method.

No blue thermoluminescence peaks were detected. Either the trapped holes are stable only below 77 K or hole detrapping occurred at a temperature when Ti^{4+} CT emission is too weak to be observed (note that the CT emission could be measured at LNT but not at RT in the photoluminescence experiment).

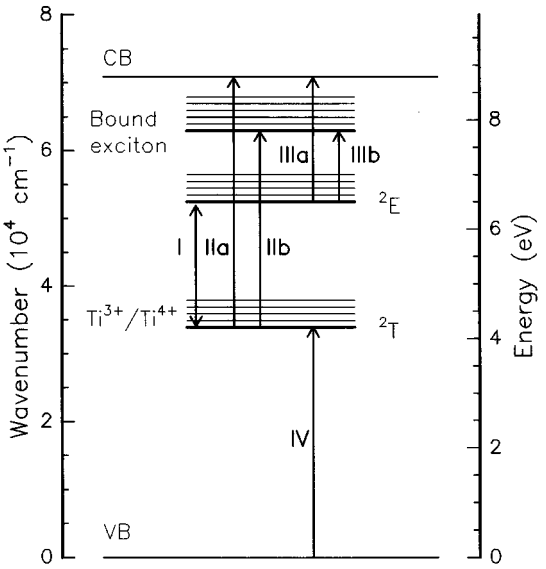

FIG. 11. Band scheme and charge-transfer transitions in $YAlO_3$:Ti. (I) $^2T \rightarrow {}^2E$ ZPL at 18 530 cm^{-1}. (IIa) threshold of UV PC tail, (IIb) onset of the UV1. (IIIa) onset of photoionization cross section from ^2E, (IIIb) onset of ESA (they both are estimated from UV data). (IV) onset of the UV2.

C. Position of Ti^{3+} levels in the band gap of $YAlO_3$

Using the values of photoionization thresholds in donor-type and in acceptor-type transitions, it is possible to find the position of the Ti^{3+}/Ti^{4+} level in the band gap of $YAlO_3$ crystals as shown in Fig. 11. Thick horizontal lines represent the zero-vibrational energy levels of the relaxed Ti electronic states. Besides the ^2T and ^2E levels of Ti^{3+}, the energies of the CB and VB edges as well as the bound exciton states are also shown. Thin horizontal lines represent the higher vibrational levels in different electronic states. The vertical arrows correspond to the pure electronic transitions whose energies were estimated from the experiments.

Since the sum of the zero-phonon donor and acceptor energies should equal the band-gap energy,

$$E_d + E_a = E_g, \tag{5}$$

we can test the values of E_d and E_a from these experiments to see if they are consistent with this relation.

The band-gap energy comes from Refs. 21–24, and especially a paper by Lushchik *et al.*[24] In this paper, a value of $E_g = 8.5$ eV is given; however the data shown permit a range from 8.5 to 9.0 eV to be chosen.

The value of E_a from Sec. III B is 4.2 ± 0.1 eV; the value of E_d from Sec. III A is 4.6 ± 0.1 eV, giving the value of E_g as 8.8 ± 0.2 eV. The value is in good agreement with the range of values for E_g indicated above.

IV. CONCLUSIONS

Through the results of spectroscopic investigations and photoconductivity measurements, the Ti^{3+} ground state is found to be at about 37 000 cm^{-1} below the conduction band of $YAlO_3$. A titanium-bound exciton band beginning at about 29 000 cm^{-1} above the Ti^{3+} ground state is observed. The charge-transfer transition from Ti^{4+} to Ti^{3+} ground state is located at $33\,900 \pm 1000$ cm^{-1} above the valence band of $YAlO_3$. The two quantities, 37 000 and 33 900 cm^{-1} sum to 70 900 cm^{-1} = 8.8 eV, close to the band-gap energy of $YAlO_3$. The result is similar to the case of Al_2O_3:Ti.[20] On the other hand, the separation between the conduction band and the ^2E excited state (18 500 cm^{-1}) is near to the $^2E \leftrightarrow {}^2T$ zero-phonon energy (18 530 cm^{-1}) of Ti^{3+} and this is the source of the ESA. The close coincidence between the excited-state ionization energy and the zero-phonon level shows that special long-wavelength pumping (wing-pumping) would be necessary if this crystal is to be used as a solid-state laser. Though a strong reduction in the pumping efficiency is still expected.

ACKNOWLEDGMENTS

Work at St. Petersburg and Hamburg was supported by the VW foundation under Grant No. I/68515. Work at Princeton was supported in the National Science Foundation under Grant No. EAR 89-17292 and the Department of Chemistry. S.B. acknowledges with thanks a grant from the program: Cooperation in Applied Science and Technology (CAST), administered by the National Research Council.

[1] R. Diehl and G. Brandt, Mater. Res. Bull. **10**, 85 (1975).
[2] T. Wegner and K. Petermann, Appl. Phys. B **49**, 275 (1989).
[3] K. Petermann, Opt. Quant. Electron. **22**, 199 (1990).
[4] M. Yamaga, Y. Gao, F. Rasheed, K. P. O'Donnell, B. Henderson, and B. Cockayne, Appl. Phys. B **51**, 329 (1990).
[5] M. Yamaga, B. Henderson, and K. P. O'Donnell, Appl. Phys. B **52**, 122 (1991).
[6] M. Yamaga, B. Henderson, K. P. O'Donnell, F. Rasheed, Y. Gao, and B. Cockayne, Appl. Phys. B **52**, 225 (1991).
[7] M. Yamaga, T. Yosida, B. Henderson, K. P. O'Donnell, and M. Date, J. Phys. Condens. Matter **4**, 7285 (1992).
[8] T. Danger, K. Petermann, and G. Huber, Appl. Phys. A **57**, 309 (1993).
[9] J. Kvapil, M. Koselja, Ji. Kvapil, B. Perner, V. Skod, J. Kubelka, K. Hamal, and V. Kubacak, Czech. J. Phys. B **38**, 237 (1988).
[10] J. Kvapil, M. Kozelja, Ji. Kvapil, and K. Hamal, in *Conference on Lasers and Electro-Optics 1989*, Technical Digest Series Vol. 11 (Optical Society of America, Washington D.C., 1989), pp. 6–8.
[11] D. S. McClure and C. Pedrini, Phys. Rev. B **32**, 8465 (1985).
[12] W. C. Wong, D. S. McClure, S. A. Basun, and M. R. Kokta, Phys. Rev. B **51**, 5693 (1995).
[13] B. D. Evans, J. Lumin. **60&61**, 620 (1994).
[14] C. Pedrini, D. S. McClure, and C. H. Anderson, J. Chem. Phys. **70**, 4959 (1979).
[15] H. Manaa, C. Pedrini, and R. Moncorge, in *OSA Proceedings on Advanced Solid-State Lasers 1991*, edited by G. Dube and L. Chase (Optical Society of America, Hilton Head, 1991), Vol. 10, pp. 371–375.
[16] S. A. Basun, A. A. Kaplyanskii, B. K. Sevastyanov, L. S. Staros-

tina, S. P. Feofilov, and A. A. Chernyshev, Fiz. Tverd. Tela **32**, 1898 (1990) [Sov. Phys. Solid State **32**, 1109 (1990)].

[17] S. A. Basun, S. P. Feofilov, A. A. Kaplyanskii, B. K. Sevastyanov, M. Yu. Sharonov, and L. S. Starostina, J. Lumin. **53**, 28 (1992).

[18] S. A. Basun, S. P. Feofilov, A. A. Kaplyanskii, T. Danger, G. Huber, and K. Petermann, in *OSA Proceedings on Advances Solid-State Lasers 1993*, edited by A. A. Pinto and T. Y. Fan (Optical Society of America, New Orleans, 1993), Vol. 15, p. 339.

[19] S. A. Basun, A. A. Kaplyanskii, O. K. Mel'nikov, B. K. Sevastyanov, and S. P. Feofilov, Fiz. Tverd. Tela **36**, 1451 (1994) [Phys. Solid State **36**, 794 (1994)].

[20] W. C. Wong, D. S. McClure, S. A. Basun, and M. R. Kokta, Phys. Rev. B **51**, 5682 (1995).

[21] V. N. Abramov and A. I. Kuznetzov, Fiz. Tverd. Tela **20**, 689 (1978) [Sov. Phys. Solid State **20**, 399 (1978)].

[22] A. I. Kuznetzov, V. N. Abramov, V. V. Murk, and B. R. Namozov, Eesti Tead. Akad. Füüs. Inst. Urim. **63**, 19 (1989).

[23] T. Tomiki, M. Kaminao, Y. Tanahara, T. Futtemma, M. Fujisawa, and F. Fukudome, J. Phys. Soc. Jpn. **60**, 1799 (1991).

[24] Ch. Lushchik, E. Feldback, A. Frorip, M. Kirm, A Lushchik, A. Maaros, and I. Martinson, J. Phys. Condens. Matter **6**, 11 177 (1994).